An Analog Neural Oscillator Circuit for Locomotion Controller in Quadruped Walking Robot

Kazuki Nakada Tetsuya Asai Yoshihito Amemiya
Department of Electrical Engineering,
Hokkaido University,
Sapporo, 060–8628, Japan.
Email: nakada,asai,amemiya@sapiens-ei.eng.hokudai.ac.jp

***Abstract*— In this report, we propose an analog neural oscillator circuit for a locomotion controller in a quadruped walking robot. Animal locomotion, such as walking, running, swimming and flying, is based on periodic rhythmic movements. These rhythmic movements are driven by the biological neural network, called the central pattern generator (CPG). In recent years, many researchers have applied CPG to the locomotion controller for walking robots. However, most of the CPG controllers have been developed with digital processors, and thus have several problems, such as high power consumption. Hence, we designed an analog circuit as a neural oscillator underlying a CPG controller. The proposed circuit is based on the Amari-Hopfield model, which is suitable for analog circuit implementation because of its simple transfer function. Furthermore, the proposed circuit operates in the subthreshold region. As a result, it can reduce power consumption. By numerical analysis, simulations and experiments, the proposed circuit is shown to have the capability to generate stable rhythmic patterns in noisy environments.**

I. Introduction

Animal locomotion, such as walking, running, swimming and flying, is based on periodic rhythmic movements. These rhythmic movements are driven by the biological neural network, called the central pattern generator (CPG) [1]. CPG consists of sets of neural oscillators, situated in ganglion or spinal cord. Induced by tonic inputs from command neurons, CPG generates a rhythmic pattern of neural activity unconsciously and automatically. As a result of such a rhythmic pattern activating the motor neurons, the rhythmic movements of animals are driven. While not necessary for generating rhythmic movements, sensory feedback regulates the frequency and phase of these rhythmic patterns generated by CPG [2]. Furthermore, CPG can adapt to various environments to change the periodic rhythmic pattern itself[1]. For instance, vertebrates, such as horses and cats, can change their locomotor patterns depending on the situation [3]. Since the coordination of physical parts is required to achieve smooth locomotion, the rhythmic movements driven by the CPG play one of the most important roles in locomotion.

In recent years, many researchers have applied CPG to locomotion control in robotics [6]-[10]. For example, quadruped robots capable of adaptating to irregular terrain using CPG dynamics have been developed by Kimura *et. al* [6]. Billard and Ijspeert have applied a CPG controller to an entertainment robot, AIBO [7]. Shan and Nagashima have proposed a CPG controller for a humanoid robot [8].

In robotics, using CPG for locomotion control has the following advantages: i) The amount of calculation required for movement control is reduced as a result of the coordination of physical parts induced by the rhythmic movements, ii) As a result of synaptic plasticity changing the structure of the CPG and the rhythmic pattern, high autonomous adaptation to various environments is achieved.

In this report, we propose an analog neural oscillator circuit underlying a CPG controller. Although a number of the CPG controllers have been developed, most of these are implemented by using digital processors [6]-[8]. While the digital processor can operate with high accuracy, it consumes high power and requires a large area of a chip. Such problems degrade the CPG controller. In order to overcome such problems, we designed an analog circuit as a neural oscillator underlying a CPG controller. Since the proposed circuit operates in the subthreshold region, it can reduce power consumption. Furthermore, we constructed a CPG controller from the proposed circuit aiming at the coordination of physical parts in a quadruped walking robot. By numerical analysis, experiments and simulations, we confirm the operation of the proposed circuit.

II. Neural Control of Rhythmic Movements

The rhythmic movements of animals, such as locomotion and breathing, are driven by CPG. CPG generates a periodic rhythmic pattern of nerve activity that activates motor neurons, with the result that rhythmic movements of animals are driven. The periodic rhythmic pattern of nerve activity can be regarded as an attractor like a limit cycle, embedded in the network structure of CPG. Characteristics of the rhythmic pattern as an attractor contribute to the stability of the rhythmic movements.

In vertebrate locomotion, one of the most fundamental roles of CPG is to control each limb. As a result of the interaction with CPGs that actuate each of the joints, the rhythmic movements of each limb are stabilized. Another role is cooperation between the limbs, i.e., interlimb coordination. Since the degree of freedom of the physical parts relevant to locomotion is very high, the coordination of physical parts is required to achieve smooth locomotion. Interlimb coordination is induced by the periodic rhythmic movements driven by CPG. Therefore, CPG can be said to play the central role in locomotion.

0-7803-7898-9/03/$17.00 ©2003 IEEE

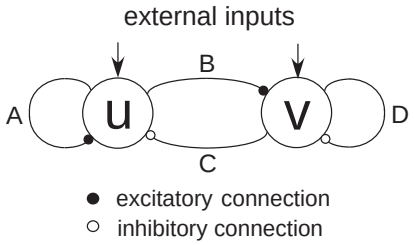

Fig. 1. The configuration of the Amari-Hopfield model

In the locomotion of mammals, transitions of the rhythmic movements are often observed. As a typical example, the horse has chosen a locomotor pattern called the gait. It is believed that optimal gait pattern has been chosen based on locomotor speed or the rate of energy consumption [3]. Such a transition of rhythmic movements is also controlled by CPG. In addition, each of the gait patterns, such as walk, trot and gallop, is characterized by the relative phase between each limb. It is considered that the transitions of the rhythmic movements are performed as a result of the regulation of the relative phase by CPG. Recently, it has been considered that substantial network structure of CPG is changed because of the synaptic strength being modulated by a neurotransmitter. As a result, CPG regulates rhythmic movements and coordination of physical parts is also changed.

III. The CPG Model

In this section, we describe a CPG model underlying the locomotion controller.

A. Neural Oscillator Model

A number of artificial neural networks have been proposed as the CPG model [4]-[5]. In the earliest research, Brown proposed the most fundamental CPG model using the neural oscillator, which consists of two neurons and has interactions between neurons by reciprocal inhibition [1]. The model is also one of the relaxation oscillators. Although its configuration is very simple, it is essential as the component of the CPG model.

In the present work, we chose the Amari-Hopfield model [12] as the neural oscillator. The model consists of an excitatory neuron and an inhibitory neuron with excitatory inhibitory connections (Fig. 1). The dynamics of the Amari-Hopfield model is expressed by the following equations:

$$\begin{cases} \tau \dot{u} = -u + A \cdot f_\mu(u) - C \cdot f_\mu(v) + S_u(t) \\ \tau \dot{v} = -v + B \cdot f_\mu(u) - D \cdot f_\mu(v) + S_v(t) \end{cases} \quad (1)$$

where u and v express the activities of the excitatory neurons and the inhibitory neurons, respectively. The parameters A, B, C and D determine the dynamics of the model. $S_u(t)$ and $S_v(t)$ express the external inputs. The transfer function $f(x)$ is given by the following equation:

$$f_\mu(x) = \frac{1 + \tanh(\mu x)}{2} \quad (2)$$

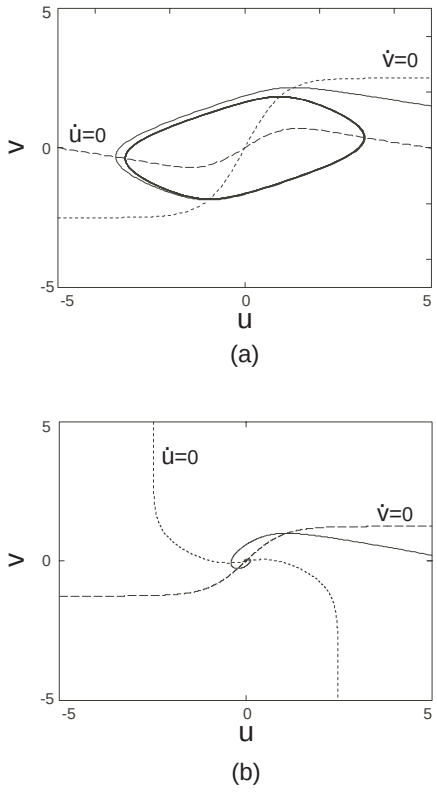

Fig. 2. The attractor of the Amari-Hopfield model in the u-v phase plane. (a) The limit cycle: $A = C = 10.0, B = 5.0, D = 0.0, S_u = 0.0, S_v = -2.5$ and $\mu = 1.0$. (b) The stable equilibrium: $A = C = 2.5, B = 2.5, D = 0.0, S_u = 0.0, S_v = -1.25$ and $\mu = 1.0$.

where $\tanh(x)$ is the hyperbolic tangent function and μ is its control parameter. The Amari-Hopfield model is suitable for implementation of the CPG model as analog circuits because of its simple transfer function. Its details are given in the following section. Furthermore, the Amari-Hopfield model corresponds to the Affine Transformation of the Wilson-Cowan model, which imitates the population activities of cortical neurons [13]. Therefore, the qualitative property of both models is equivalent. The dynamics of both models have been studied in detail. Depending on the parameters A through D and the external inputs $S_u(t)$ and $S_v(t)$, the Amari-Hopfield model generates the periodic pattern automatically. Figures 2(a) and 2(b) show the dynamics of the Amari-Hopfiled model in the *u-v* phase plane.

B. Neural network model

We composed a neural network model as the CPG controller to perform interlimb coordination. As the CPG controller for interlimb coordination, it is desirable to generate various rhythmic patterns. Hence, we constructed a neural network model from the Amari-Hopfield model according to the neural network proposed by Nagashino *et al* [11]. Their model consists of four coupled neural oscillators with excitatory and inhibitory interneurons. As a result of introducing the interneurons and controlling their interactions with neural oscillators,

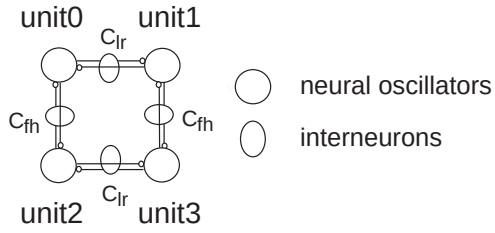

Fig. 3. The basic configuration of the network

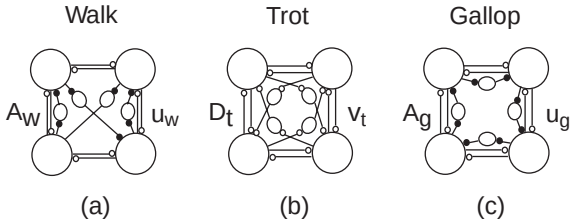

Fig. 4. The configurations of the networks correspond to the typical gait patterns. (a) the walk mode. (b) the trot mode. (c) the gallop mode.

substantial network structure is changed and various rhythmic patterns are generated [11].

Figure 3 shows the basic structure of the neural network model. Here, we describe configurations of networks that generate periodic rhythmic patterns corresponding to each of the typical gaits of mammals. Figures 4(a), (b) and (c) correspond to the walk mode, the trot mode and the gallop mode, respectively [11].

By combining the networks that correspond to each of the gait modes, we construct the entire network. The network dynamics are given by the following equations:

$$\begin{aligned}\tau_u \dot{u}^{\{0,1,2,3\}} = &-u^{\{0,1,2,3\}} + Af_\mu(u^{\{0,1,2,3\}}) \\ &+A_w f_\mu(u_w^{\{2,3,1,0\}}) + A_g f_\mu(u_g^{\{2,0,3,1\}}) \\ &-C_{lr} f_\mu(v^{\{1,0,3,2\}}) - C_{fh} f_\mu(v^{\{2,3,0,1\}}) \\ &-Cf_\mu(v^{\{0,1,2,3\}}) + I_u^{\{0,1,2,3\}}(t)\end{aligned} \tag{3}$$

$$\begin{aligned}\tau_v \dot{v}^{\{0,1,2,3\}} = &-v^{\{0,1,2,3\}} + Bf_\mu(u^{\{0,1,2,3\}}) \\ &-D_t f_\mu(v_t^{\{3,2,1,0\}}) + I_v^{\{0,1,2,3\}}(t)\end{aligned} \tag{4}$$

$$\begin{aligned}\tau_w \dot{u}_w^{\{0,1,2,3\}} = &-u_w^{\{0,1,2,3\}} + A_w f_\mu(u^{\{0,1,2,3\}}) \\ &+I_{uw}^{\{0,1,2,3\}}(t)\end{aligned} \tag{5}$$

$$\begin{aligned}\tau_g \dot{u}_g^{\{0,1,2,3\}} = &-u_g^{\{0,1,2,3\}} + A_g f_\mu(u^{\{0,1,2,3\}}) \\ &+I_{ug}^{\{0,1,2,3\}}(t) + I_{xg}^{\{0,1,2,3\}}(t)\end{aligned} \tag{6}$$

$$\begin{aligned}\tau_t \dot{v}_t^{\{0,1,2,3\}} = &-v_t^{\{0,1,2,3\}} - D_t f_\mu(v^{\{0,1,2,3\}}) \\ &+I_{vt}^{\{0,1,2,3\}}(t) + I_{xt}^{\{0,1,2,3\}}(t)\end{aligned} \tag{7}$$

where the numbers correspond to each unit, u, u_w and u_g represent activities of the excitatory neurons, v and v_t represent activities of the inhibitory neurons, $\tau_u, \tau_v, \tau_{u_w}, \tau_{u_g}$ and τ_{v_t} are the time constant of the neuros, $A, A_w, A_g, B, C, C_{lr}, C_{fh}$ and D_t are the interaction parameters. $I_u, I_v, I_{u_w}, I_{u_g}$ and I_{v_t} are the tonic bias inputs, and I_{x_w} and I_{w_g} are the external inputs.

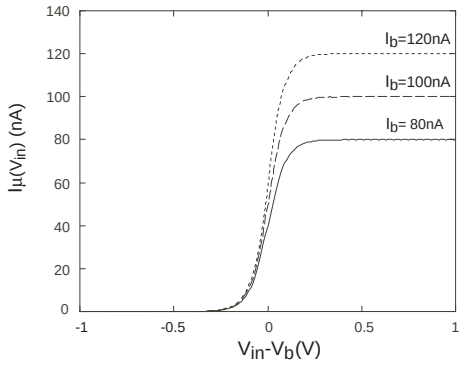

Fig. 5. The static response of the differential pair.

IV. The CPG Controller

In this section, the neural oscillator circuit underlying the CPG controller is described, and we construct the CPG controller from the neural oscillator circuit.

A. Neural Oscillator Circuit

First, we describe the characteristics of the differential pair, which is one of the most fundamental components of the neural oscillator circuit. The differential pair can approximate the transfer function. When the MOS transistors, which comprise the differential pair, operate in their subthreshold region, the static response of the differential pair (Fig. 5) is given by the following equation [14]:

$$I_\mu(v) = I_b \frac{1 + \tanh(\mu(v - v_b))}{2} \tag{8}$$

where v is the input voltage, v_b is the bias voltage, $\mu = \kappa/2V_T$, V_T is the thermal voltage, I_b is the bias current and κ is the device parameter.

The excitatory cell circuit is shown in Fig. 6(a). It consists of the RC circuit, the differential pair and the current source. The dynamics of the excitatory cell is given by the following equation:

$$C_u \dot{u} = -\frac{u}{R_u} + I_u(t) \tag{9}$$

where u expresses the voltage value, C_u is the capacitance value, R_u is the resistance value and $I_u(t)$ is the external current. The excitatory cell outputs positive current according to (8).

The inhibitory cell circuit is shown in Fig. 6(b). It also consists of the RC circuit, the differential pair and the current source. The dynamics of the inhibitory cell is given by the following equation:

$$C_v \dot{v} = -\frac{v}{R_v} + I_v(t) \tag{10}$$

where v expresses the voltage value, C_v is the capacitance value, R_v is the resistance value and $I_v(t)$ is the external current. The inhibitory cell outputs negative current according to (8).

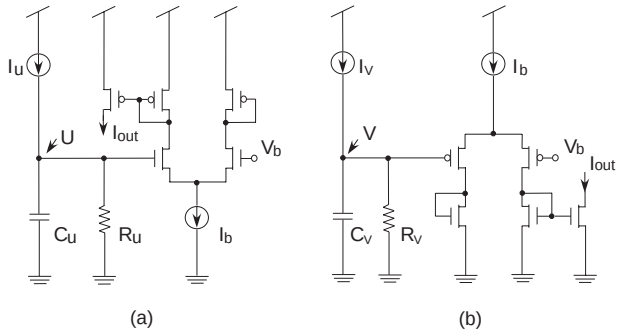

Fig. 6. The schematic of the inhibitory circuit.

The neural oscillator circuit is constructed from the excitatory circuit and the inhibitory circuit (Fig. 7), and its dynamics is given by rewriting (1) as follows:

$$\begin{cases} C_u\dot{u} = -\dfrac{u}{R_u} + A{\cdot}I_\mu(u) - C{\cdot}I_\mu(v) + I_u(t) \\ C_v\dot{v} = -\dfrac{v}{R_v} + B{\cdot}I_\mu(u) + I_v(t) \end{cases} \tag{11}$$

where the parameters A through C are the same as in (1), and $I_\mu(u)$ and $I_\mu(v)$ are the output currents of the differential pairs. The circuit generates periodic rhythmic patterns, depending on the parameters A through C and the external inputs $I_u(t)$ and $I_v(t)$.

B. The Network Circuit

We constructed the CPG network circuit from the neural oscillator circuit. Here, we use the excitatory cell as the excitatory interneurons and the inhibitory cell as the inhibitory interneuros. Let us rewrite (3)-(7) as follows:

$$\begin{aligned} C_u\dot{u}^{\{0,1,2,3\}} = &-\frac{u^{\{0,1,2,3\}}}{Ru} + AI_\mu(u^{\{0,1,2,3\}}) \\ &+A_wI_\mu(u_w^{\{2,3,1,0\}}) + A_gI_\mu(u_g^{\{2,0,3,1\}}) \\ &-C_{lr}I_\mu(v^{\{1,0,3,2\}}) - C_{fh}I_\mu(v^{\{2,3,0,1\}}) \\ &-CI_\mu(v^{\{0,1,2,3\}}) + I_u^{\{0,1,2,3\}} \end{aligned} \tag{12}$$

$$\begin{aligned} C_v\dot{v}^{\{0,1,2,3\}} = &-\frac{v^{\{0,1,2,3\}}}{Rv} + BI_\mu(v^{\{0,1,2,3\}}) \\ &-D_tI_\mu(v_t^{\{3,2,1,0\}}) + I_v^{\{0,1,2,3\}} \end{aligned} \tag{13}$$

$$\begin{aligned} C_w\dot{u}_w^{\{0,1,2,3\}} = &-\frac{u_w^{\{0,1,2,3\}}}{Ru_w} + A_wI_\mu(u^{\{0,1,2,3\}}) \\ &+I_{uw}^{\{0,1,2,3\}} \end{aligned} \tag{14}$$

$$\begin{aligned} C_g\dot{u}_g^{\{0,1,2,3\}} = &-\frac{u_g^{\{0,1,2,3\}}}{Ru_g} + A_gI_\mu(u^{\{0,1,2,3\}}) \\ &+I_{ug}^{\{0,1,2,3\}} \end{aligned} \tag{15}$$

$$\begin{aligned} C_t\dot{v}_t^{\{0,1,2,3\}} = &-\frac{v_t^{\{0,1,2,3\}}}{Rv_t} - D_tI_\mu(v^{\{0,1,2,3\}}) \\ &+I_{vt}^{\{0,1,2,3\}} + I_{xt}^{\{0,1,2,3\}} \end{aligned} \tag{16}$$

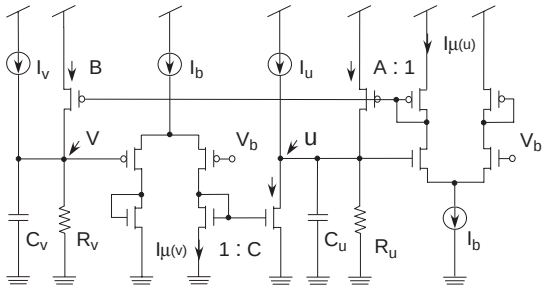

Fig. 7. The schematic of the neural oscillator circuit.

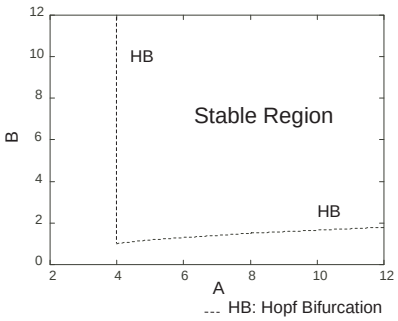

Fig. 8. The bifurcation diagram of the Amari-Hopfield model.

where $I_\mu(\cdot)$ is the output current of the differential pair. The capacitance values C_u through C_{vt}, the resistance values R_u through R_{vt}, and the interaction parameters A through D_t correspond to those in equations (3)-(7). I_u, I_v, I_{uw}, I_{ug}, I_{vt} and I_{xt} are the DC bias currents. The ratio of the interaction parameters is determined by the aspect ratio W/L (W: the gate width, L: the gate length) of the transistors, which comprise the current mirrors in the circuits. These values are determined by the bias currents of the differential pairs. Depending on interaction parameters A through D_t, the rhythmic pattern corresponding to each gait pattern is generated.

V. Results

In this section, we confirm the operation of the proposed circuit.

A. Stability Analysis

In order to determine the interaction parameters of the neural oscillator circuit, we examined the stability of the periodic solution in the Amari-Hopfield model. By numerical analysis using the dynamical system package AUTO [15], we obtained the bifurcation diagram shown in Fig. 8. Here, in order to simplify analysis, the parameters in (1) were set as follows:

$$D = 0.0,\ S_u = 0.0,\ S_v = B/2,\ \mu = 1.0 \tag{17}$$

Furthermore, we fixed the interaction parameters at $A = C$.

Generally, a stable periodic solution is created at Hopf bifurcation. Therefore, we can obtain a stable periodic solution as a result of setting the interaction parameters at the stable region in the bifurcation diagram.

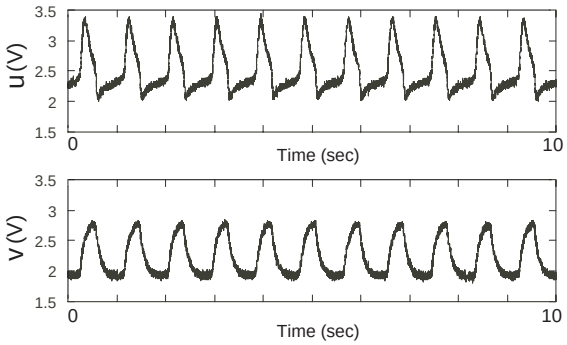

Fig. 9. The waveforms of the voltage u and v.

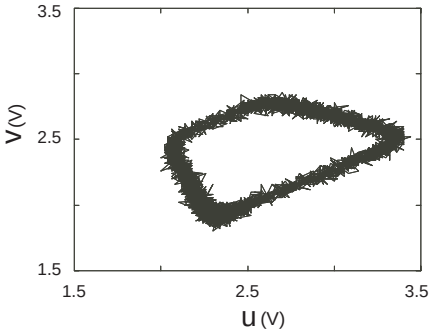

Fig. 10. The limit-cycle in the u-v phase plane.

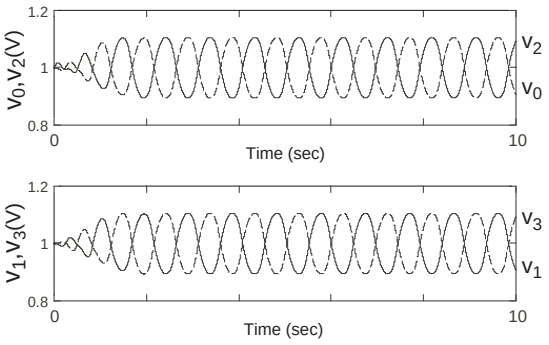

Fig. 11. The waveforms correspond to the Trot mode.

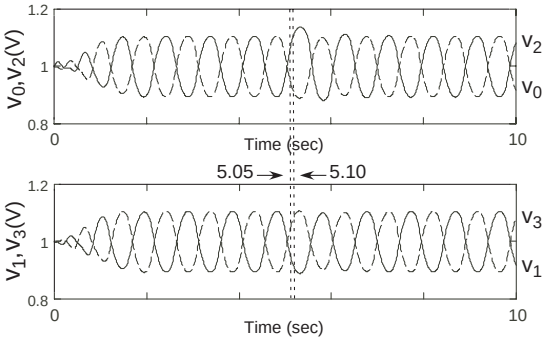

Fig. 12. The waveforms with the turbulence in the Trot mode.

B. Experiments

Depending on the interaction parameters determined by the bifurcation diagram, the neural oscillator circuit is implemented on the breadboard. We used the nMOS FET (2SK1398) and pMOS FET (2SJ184) [16]. We set the interaction parameters at:

$$A = C = 10.0,\ B = 5.0,\ D = 0.0 \tag{18}$$

The resistance values R_u and R_v were set at 1 MΩ, the capacitance values C_u and C_v were set at 100 μF, the bias currents I_b, I_u and I_v were set at (1.0, 2.5, 2.0) μA and the bias voltage V_b was set at 2.5 V. The parasitic capacitance in the breadboard can be ignored since it is fully smaller than the capacitance values C_u and C_v.

We measured the voltage value u and v in the circuit. As a result, we obtained the waveforms shown in Fig. 9. The dynamics of the circuit in the u-v phase plane are shown Fig. 10. Although additive noise existed (SNR: 30db), a stable periodic pattern of the voltage u and v was obtained.

C. Simulations

We confirmed the operation of the network circuit through computer simulation. In the following simulation, we used the circuit simulator PSPICE and assumed 1.5-μm CMOS device technology. As typical device parameters, $I_0 = O(10^{-16})$ A and $\kappa = 0.6$ were assumed. As common parameters, the gate length L = 1.5 μm, the capacitance values C_u, C_v, C_{ug}, C_{vt} and C_{uw} were set at (100, 100, 100, 100, 300) nF and the resistance values $R_u, R_v, R_{u_w}, R_{u_g}$ and R_{v_t} were set at 1 MΩ. The interaction parameters A, B, C, C_{lr} and C_{fh} were set as follows:

$$A = C = 4.0,\ B = 3.0,\ C_{lr} = C_{fh} = 1.0$$

Furthermore, we set the bias currents in the differential pairs I_b at 100 nA.

First, we confirmed the generation of the periodic rhythmic patterns in the circuit. In particular, we show an example of the rhythmic patterns generated by the circuit in Trot mode. We set the parameters as follows:

$$D_t = 1.0,\ A_w = A_g = 0.0$$

where we cut off the output currents of the interneurons u_w and u_g by using switch in order to set the interaction parameters at 0. The bias voltage v_b = 1.0 V, the bias currents I_b = 100 nA, the bias currents I_u^k, I_v^k, I_{uw}^k, I_{ug}^k, and I_{vt}^k $(k = 0, 1, 2, 3)$ were set at (950, 550, 750, 750, 850) nA and the bias currents I_{xt}^0 I_{xt}^1 I_{xt}^2 and I_{xt}^3 were set at (10, 0, 0, 10) nA. The periodic rhythmic patterns of $v^{\{0,1,2,3\}}$ are shown in Fig 11.

We confirmed the stability of the circuit in the Trot mode. In Fig. 12, we introduce weak current (900 nA) as disturbance to the circuit at 5.05 sec to 5.10 sec. The circuit is stable against this disturbance. It is assumed that this stability is provided by the characteristics of the rhythmic patterns as the attractor of the network. If disturbance is considered to be an input from

a sensory neuron, the phase of the periodic pattern would be regulated by sensory feedback.

D. Discussion

As a result of numerical analysis, simulations and experiments, we confirmed the performance of the proposed circuit. In particular, we confirmed that the proposed circuits are stable against additive noise and weak disturbance. This characteristic is suitable for the CPG controller in a quadruped walking robot.

VI. CONCLUSION

In this paper, we proposed an analog neural oscillator circuit for a locomotion controller in a quadruped walking robot. The proposed circuit is based on the biological neural network, called CPG. In recent years, many researchers have applied CPG to locomotion controllers in robotics. However, most of the CPG controllers have been developed using digital processors that have several problems, such as high power consumption. In order to improve such problems, we designed an analog neural oscillator circuit underlying the CPG controller. The proposed circuit is based on the Amari-Hopfield model, which is suitable for analog circuit implementation because of its simple transfer function. Therefore, the circuit consists of the most fundamental analog circuit, such as the differential pair, the current mirror and the RC circuit. Since MOS transistors, which comprise the proposed circuit, operate in their subthreshold region, it can reduce power consumption. Furthermore, we construct the CPG controller from the neural oscillator circuit, aiming at the interlimb coordination of a quadruped walking robot.

By numerical analysis, computer simulations and experiments, we confirmed the operation of the proposed circuit. As a result, it is shown that the proposed circuit has the capability to generate stable rhythmic patterns in noisy environments.

Our future work will aim to develop an analog CPG controller for an autonomous micro locomotor robot.

REFERENCES

[1] F. Delcomyn, *Foundations of Neurobiology*, W.H. Freeman and Co, New York, 1997.

[2] *The Handbook of Brain Theory and Neural Networks, Second Edition*.M. Arbib Ed., USA, MIT PRESS, Press 2002.

[3] J. Nishii, "Legged animals select the optimal locomotor pattern based on energetic cost," *Biological Cybernetics*., vol.83, pp.435-442, 2000.

[4] K. Matsuoka, "Mechanism of Frequency and Pattern Control in the Neural Rhythm Generators," *Biological Cybernetics*., vol,56, pp.345-353, 1987.

[5] G. Taga, Y. Yamaguchi and H. Shimizu, "Self-organized control of bipedal locomotion by neural oscillators in unpredictable environment," *Biological Cybernetics*., vol. 65, pp.147-159, 1991.

[6] H. Kimura, Y. Fukuoka and K. Konaga, "Adaptive Dynamic Walking of a Quadruped Robot by Using Neural System Model," *ADVANCED ROBOTICS*, Vol.15, No.8Cpp.859-876, 2001.

[7] A. J. Ijspeert and A. Billard, "Biologically inspired neural controllers for motor control in a quadruped robot," In *proc, International Joint Conference on Neural Network conference.*, 2000.

[8] J. Shan, F. Nagashima, "Neural Locomotion Controller Design and Implementation for Humanoid Robot HOAP-1", In *proc. The 20th RSJ conference*, 2002.

[9] G. Patel, J. Hollemam and S. Deweerth, "Analog VLSI Model of Intersegmental Coordination with Nearest Neighbor Coupling," In *Adv. Neural Information Processing*., vol. 10, pp.710-725, 1998.

[10] M. A. Lewis, M. J. Hartmann, R. Etienne-Cummings, A. H. Cohen, "Control of a robot leg with an adaptive aVLSI CPG chip", *Neurocomputing*., vol.38-40, pp 1409-1421, 2001.

[11] H.Nagashino, Y. Nomura and Y. Kinouchi. "Generation and Transitions of Phase-Locked Oscillations in Coupled Neural Oscillators", In *proc, The fortieth SICE Annual Conference*, 2001.

[12] S. Amari, "Characteristic of the random nets of analog neuron-like elements," *IEEE trans. on System, Man and Cybernetics*, SMC-2, pp.643-657, 1972.

[13] H. R. Wilson and J. D. Cowan, "Excitatory and Inhibitory interactions in localized populations of model neurons," *Biophys. J.*, Vol. 12, pp.1-24, 1972.

[14] C. A. Mead, *Analog VLSI and Neural Systems*, Reading, Mass, Addison-Wesley, 1989.

[15] E. Doedel, X. Wang, and T. Fairgrieve, "Auto94: Software for continuation and bifurcation problems in ODEs," Appl. Math. Technical Report, California Inst. of Technology, 1994.

[16] http://www.necel.com/discrete/japanese/document/mosfet.html